Howard Hughes Medical Institute

Published as: *Nat Methods*. 2018 November ; 15(11): 936–939.

Stability, affinity and chromatic variants of the glutamate sensor iGluSnFR

Jonathan S. Marvin[1], **Benjamin Scholl**[2], **Daniel E. Wilson**[2], **Kaspar Podgorski**[1], **Abbas Kazemipour**[1,11], **Johannes Alexander Müller**[3], **Susanne Schoch**[3], **Francisco José Urra Quiroz**[4], **Nelson Rebola**[4], **Huan Bao**[5], **Justin P. Little**[1,6], **Ariana N. Tkachuk**[1], **Edward Cai**[1,10], **Adam W. Hantman**[1], **Samuel S.-H. Wang**[7], **Victor J. DePiero**[8], **Bart G. Borghuis**[8], **Edwin R. Chapman**[5], **Dirk Dietrich**[9], **David A. DiGregorio**[4], **David Fitzpatrick**[2], and **Loren L. Looger**[1,*]

[1]Howard Hughes Medical Institute (HHMI), Janelia Farm Research Campus, Ashburn, Virginia, USA

[2]Max Planck Florida Institute for Neuroscience, Jupiter, Florida, USA

[3]Department of Neuropathology, University of Bonn, Bonn, Germany

[4]Unit of Dynamic Neuronal Imaging and Centre National de la Recherche Scientifique, Institut Pasteur, Paris Cedex 15, France

[5]Department of Neuroscience, HHMI, University of Wisconsin–Madison, Madison, Wisconsin, USA

[7]Department of Molecular Biology, Princeton Neuroscience Institute and Princeton University, Princeton, New Jersey, USA

[8]Department of Anatomical Sciences and Neurobiology, University of Louisville School of Medicine, Louisville, Kentucky, USA

[9]Department of Neurosurgery, University of Bonn, Bonn, Germany

---

*corresponding author: loogerl@janelia.hhmi.org.
[6]current address: New York University Langone Health, Department of Radiology, New York, New York, USA
[10]current address: Department of Biomedical Engineering, Johns Hopkins University, Baltimore, Maryland, USA
[11]current address: Department of Neurobiology, Stanford University, Stanford, California, USA

Author contributions

JSM and LLL: Protein engineering and manuscript; BS, DEW, and DF: Ferret visual cortex; JAM, SS-M, and DD: Neuronal culture analysis; JPL: Brightness assessment in somatosensory cortex; KP and AK: High speed imaging of yellow variant; ANT and EC: Protein engineering; HB and ERC: Stopped-flow kinetics; NR, FJUQ, SW, AWH, DAD: Cerebellum; VJD, BGB: Retina.

Competing financial interests

Marvin and Looger have US Patent 9719992, which pertains to original iGluSnFR..

Code availability

All analysis code used in this study is available upon request.

Data availability

All data from this study is available upon request.

Accession codes

All constructs have been deposited at Addgene (#106174–106206; *hSynapsin1*, FLEX-*hSynapsin1*, FLEX-*CAG*, *GFAP* promoters; some fusions with the red fluorescent protein mRuby3 are available). Sequences have been deposited in Genbank (MH392460–5). AAV virus is available from Addgene.

Note: Supplementary information is available in the online version of the paper.

Abstract

Single-wavelength fluorescent reporters allow visualization of specific neurotransmitters with high spatial and temporal resolution. We report variants of the glutamate sensor iGluSnFR that are functionally brighter, detect sub-micromolar to millimolar glutamate, and have blue, cyan, green, or yellow emission profiles. These variants allow *in vivo* imaging where original iGluSnFR was too dim, can resolve glutamate transients in dendritic spines and axonal boutons, and permit kilohertz imaging.

The intensity-based glutamate-sensing fluorescent reporter (iGluSnFR)[1] has become an invaluable tool for studying glutamate dynamics in diverse systems, including retina[2], mouse olfactory bulb[3] and cat visual cortex[4]. iGluSnFR also allows mesoscale "functional connectomic" mapping[5] and mechanistic studies of exocytic vesicle fusion[6], synaptic spillover[7], cortical spreading depression[8] and Huntington's disease[9]. However, iGluSnFR properties are limited: too slow to follow fast synaptic transients, and too insensitive to detect very sparse release. Here we describe variants that are functionally brighter (due to increased expression), have higher or lower affinity (resulting from slower or faster off-rates), and fluoresce blue, green, or yellow.

Replacement of circularly permuted eGFP with circularly permuted superfolder GFP[10] (SF-iGluSnFR) increases the thermodynamic stability and soluble-protein expression level of iGluSnFR in bacteria, without changing the 2-photon cross-section and excitation, emission, and absorption spectra (Supp. Fig. S1).

SF-iGluSnFR expressed robustly in mouse somatosensory cortex, and was bright enough for typical resonance scanner-based 2-photon imaging *in vivo* (<20 mW at the sample, Supp. Fig. S2a,b), whereas original iGluSnFR was unobservable. When laser power was increased to make original-iGluSnFR observable (Supp. Fig. S2c,d), partially bleached SF-iGluSnFR was still brighter than unbleached original-iGluSnFR (Supp. Fig. 2e,f). Furthermore, continuous imaging of a single spine expressing SF-iGluSnFR in the barrel cortex showed negligible bleaching during a 7-minute experiment (Supp. Fig S2g). In mouse retina, where original iGluSnFR expresses well, SF-iGluSnFR was significantly more photostable (Supp. Fig. S3).

While the affinity of iGluSnFR is adequate for some *in vivo* applications, faster off-rate variants are needed to resolve fast glutamate transients associated with local glutamate release. Mutating S72 in the glutamate-binding pocket to alanine results in a soluble protein (SF-iGuSnFR.S72A) with a slower on-rate, faster off-rate, and 200 μM affinity for glutamate (Supp. Fig. S4a,b). The affinity of Venus flytrap-like binding proteins can be altered without compromising the stereochemical integrity of the ligand-binding site by making mutations to the "hinge" region and allosterically shifting the open/ligand-free to closed/ligand-bound equilibrium[11]. We screened a saturating A184X library of SF-iGluSnFR (mutated to valine, A184V, in original- iGluSnFR). Reversion to alanine or other small amino acids increased affinity (A184A had a low ΔF/F), while larger side chains decreased affinity (Supp. Fig. 4c). A184S has a slower off-rate, and increases affinity from 40 μM (A184V) to 7 μM (A184S, Supp. Fig. S4a,b).

These new SF-iGluSnFR variants (S72A (low affinity), A184V (original), and A184S (high affinity)) were re-cloned into an AAV vector containing an IgG secretion signal and a PDGFR transmembrane domain. Expression of the membrane-tethered version in cultured rat hippocampal neurons increases its affinity by an order of magnitude (Supp. Fig. S5a) as was observed with the original sensor[1]. Whole-field electrical stimulation (50 Hz) of neuronal cultures expressing SF-iGluSnFR variants prominently increased fluorescence, with decay rates that parallel the *in vitro* kinetics; all variants decayed faster than the calcium sensor GCaMP6f (Supp. Fig. S5b). (Recently, another iGluSnFR mutant at this site, S72T, was published[12]; in our hands, SF-iGluSnFR.S72T shows lower ΔF/F than S72A.)

In vivo, the low affinity SF-iGluSnFR.A184S variant improved detection of stimulus-evoked glutamate release in ferret visual cortical neuropil in response to drifting gratings (Fig. 1). In neuropil, peak amplitudes reached 30% ΔF/F for SF-iGluSnFR.A184S (Fig. 1a-c) but only 5% ΔF/F for SF-iGluSnFR.A184V (Supp. Fig. S7a-c), and were not apparent with original iGluSnFR (data not shown). Detectable, but lower-magnitude, changes in fluorescence were also seen on cell bodies with SF-iGluSnFR.A184S (Fig. 1a-c). The greater ΔF/F of SF-iGluSnFR.A184S allowed extraction of robust orientation tuning curves in regions of sparse labeling (Fig. 1d, Supp. Fig. S8). It also allowed orientation-selective responses to be resolved in individual dendritic spines, with some spillover onto nearby dendrites (Fig. 1e,f). Some individual spines showed robust orientation selectivity (Fig. 1g), while other spines on the same dendrite exhibited little or no visually-driven activity (Supp. Fig. S8c). The response magnitude at spines was stable over multiple stimulus presentations, with no appreciable loss in fluorescence intensity or ΔF/F (Supp. Fig. S7). Response amplitudes across individual trials were consistently greater than the A184V variant (Supp. Fig. S6c-e) when examining all stimulus-evoked responses (A184S median ΔF/F = 16%, n = 72 spines; A184V median ΔF/F = 9%, n = 22 spines; $p < 0.0001$, Wilcoxon rank-sum test) or only preferred stimuli (A184S median ΔF/F = 27%, n = 72; A184V median ΔF/F = 14%, n = 22; $p < 0.0001$; Supp. Fig. S8b). Single-trial responses from individual spines showed clear orientation selectivity and displayed robust glutamate events with high signal-to-noise ratio (Supp. Fig. S8d.e; Supp. Video 1).

The fast off-rate of SF-iGluSnFR.S72A can provide more accurate quantification of quantal synaptic responses at high stimulation frequencies over SF-iGluSnFR.A184V and original-iGluSnFR (Fig. 2a,b; Supp. Fig. S9). Transmitter release and its temporal depression can be decreased or increased by changing the extracellular calcium concentration[13]. SF-iGluSnFR.A184V and original-iGluSnFR could not well distinguish the differences in the temporal pattern of transmitter release between 1 mM and 3.5 mM Ca^{2+} during a brief train (20 Hz). In contrast, S72A reported the well-known conversion of facilitation of individual responses during the train to a strong depression upon switching from low to high extracellular Ca^{2+} (Fig. 2c). This makes SF-iGluSnFR.S72A more useful for assessing short-term synaptic plasticity. S72A also enhanced spatial resolution of glutamate release over A184V (Supp. Fig. S10).

We next examined whether SF-iGluSnFR could be used as an alternative to GCaMP6f for monitoring pre-synaptic activity of granule cell axons within mouse cerebellar brain slices. Axons of granule cells bifurcate in the molecular layer of the cerebellar cortex to form

parallel fibers (PFs; Fig. 2d), which can be reliably stimulated by local extracellular methods[14]. Single action potential (AP)-evoked fluorescence from SF-iGluSnFR.A184V was detected in individual PF boutons using fast linescan 2P imaging (~1 msec per line; Fig. 2e,f). Not all stimuli evoked fluorescence changes, as expected when vesicle fusion probability is low and there are few release sites[15]. This silence was not due to AP initiation failure, as our stimulation protocol reliably produced axonal Ca^{2+} transients (Supp. Fig. S11). SF-iGluSnFR showed faster rise and decay times than GCaMP6f in 2 mM extracellular calcium ($[Ca^{2+}]_e$, Fig. 2f, Supp. Fig. S12a). S72A was even faster (decay half-times: S72A, 10.6 ± 1.4 msec; A184V, 29.1 ± 1.8 msec; GCaMP6f, 111.4 ± 6.7 msec; Supp. Fig. S12a). The SNRs were largest for A184V (Fig. 2g). GCaMP6f bouton fluorescence accumulated during 20 Hz stimulation, while both A184V and S72A produced distinct responses that each returned to baseline (Fig. 2h, Supp. Fig. S12b), similar to dendritic responses in culture (Fig. 2a). Because the average of 3 to 10 fluorescence traces from a single bouton has comparable noise to 3–10 boutons averaged in one trial (Fig. 2e), we suggest that pre-synaptic action potentials could be inferred from SF-iGluSnFR responses. We analyzed population averages to demonstrate that SF-iGluSnFR variants are sufficiently fast to report single events even in response to 100 Hz stimulation, in contrast to GCaMP6f (Fig. 2h, Supp. Fig. S12c). Therefore, provided that a sufficient number of boutons from the same axon can be recorded simultaneously, SF-iGluSnFR, unlike GCaMP6f, could enable detection of PF firing frequencies typical of the high instantaneous firing rates (>100 Hz) of cerebellar granule cells[16].

Introduction of chromophore mutations from GFP variants Azurite, mTurquoise2, or Venus to SF-iGluSnFR led to functional blue, cyan, and yellow versions (Supp. Fig. S13 lists annotated amino acid sequences). SF-Azurite-iGluSnFR and SF-mTurquoise2-iGluSnFR required re-optimization to increase ΔF/F (Supp. Fig. S14). SF-Venus-iGluSnFR was a straightforward modular replacement with similar affinity and maximum fluorescence response as SF-iGluSnFR, but with red-shifted excitation and emission spectra (Supp. Fig. S14). Importantly, its 2-photon excitation spectrum allows strong excitation at 1030 nm (Supp. Fig. S14), compatible with relatively inexpensive, powerful femtosecond fiber lasers[17]. The high output power of fiber lasers enables simultaneous excitation of many foci, enabling fast (1016 Hz) imaging of large areas[18]. In neuronal culture, two near-simultaneous pulses of uncaged glutamate could be resolved with both high spatial and temporal resolution in a neuron expressing SF-Venus-iGluSnFR.A184V (Fig. 3a-b and Supp. Video 2). Propagation of fluorescence through the sample was consistent with diffusion of glutamate (Fig. 3c). In mouse visual cortex, single-spine fluorescence transients were recorded from sparsely expressed SF-Venus-iGluSnFR.A184S in response to moving gratings (Fig. 3d, Supp. Video 3). Strongly orientation-selective spines (Fig. 3e) were detected with minimal signal response from adjacent dendritic segments. SNR was sufficient to detect orientation-selective responses in single trials (Fig. 3f).

The SF-iGluSnFR variants described here increase the power of genetically encoded glutamate imaging. Affinity variants with altered kinetics broaden the dynamic and concentration range of observable glutamate transients. Chromatic mutants allow fast imaging with lower-cost lasers, and open a path to multi-color imaging in conjunction with other probes. In all applications, improvements in membrane targeting and photostability

will add precision, especially in complex tissues such as brain neuropil, where synapses outnumber neurons by a factor of thousands. Together, these variants substantially increase the potential of glutamate imaging to monitor brain function.

Online Methods

In vivo assessment of iGluSnFR brightness and photostability in apical dendrites in mouse somatosensory cortex

All procedures were approved by the Janelia Institutional Animal Care and Use Committee and Institutional Biosafety Committee. Wildtype C57BL/6J mice were purchased from the Jackson Laboratory and group housed in the Janelia animal facility. Mice (either sex) were injected at 8 weeks of age with AAV2/1.*hSynapsin1*.iGluSnFR.A184S or SF-iGluSnFR.A184S, at identical titers (1×10^{13} genomic copies per milliliter, GC/mL), volumes (20 nL), and locations (3 mm lateral to midline, 1.4 mm caudal to Bregma, and 0.3 mm below the cortical surface). After viral injection, a craniotomy (3 mm diameter) was made over the injection site, and the skull was replaced with a #1.5 Schott glass and fixed in place with dental acrylic (Lang Dental Manufacturing), which also secured a titanium head bar to the skull for head-mounting during imaging experiments.

In vivo two-photon imaging experiments were performed during a state of 'quite wakefulness', after having been habituated to head fixation the prior 2–3 days. Periodic water rewards were given to keep animals hydrated and passive. For comparisons of intensity and bleaching, we used a custom two-photon microscope emitting 960 nm light from a Coherent Chameleon ultrafast laser. All experiments were performed using a 25×, 1.05 NA Olympus objective immersed in water. Image acquisition was performed with ScanImage (Vidrio) software and analyzed post hoc using ImageJ (NIH). Images were acquired at a variety of speeds/zooms, and powers in order to assess the impact of pulse energy and dwell time on bleaching and intensity. Images at each setting were acquired for 5 seconds. To analyze the data, images were averaged and thresholded to create a signal (above threshold) and background mask. Signals in these masks were then averaged, and signal-to-noise ratio (SNR) was calculated from these as (signal-background)/(standard deviation of background). Bleaching percentage was calculated as the average intensity in the first 25% of the trace, divided by the last 25% of the trace.

Mouse retinal explant imaging for assessment of iGluSnFR brightness and photostability

Retinas were prepared using established methods[19]. iGluSnFR was expressed in retinal neurons by injecting 0.8–1.0 μL of AAV2/1.*hSynapsin1* virus (1×10^{13} GC/mL) into the vitreous humor of adult mouse eyes using a custom-designed syringe (Borghuis Instruments; New Haven, CT). After 17 – 21 days, eyes were dissected in oxygenated Ames medium (95% O_2–5% CO_2; Sigma-Aldrich) under infrared illumination (OWL Night Vision Scopes, third generation; B. E. Meyers), and each retina was removed from the sclera and mounted photoreceptor-side down on nitrocellulose paper with apertures for visual stimulation of the photoreceptors. Tissues were placed in a recording chamber on a custom-built two-photon fluorescence microscope (Olympus BX-51) and continuously perfused with oxygenated Ames medium at physiological temperature (~6 mL/min; 34 –36°C). Two-photon

fluorescence measurements were made with ScanImage software v3.6 (www.scanimage.org)[20] using an Olympus 60×, 1.0 NA, LUMPlanFl/IR objective and an ultra-fast pulsed laser (Chameleon Vision II; Coherent) tuned to 927 nm. Images (512×128 pixels) were acquired at 16 frames per second; line scans were obtained at 2 kHz and down-sampled (box-car average) to 500 Hz for presentation in Supp. Fig. S3. Visual stimuli were generated with an Apple iMac computer using Matlab (The MathWorks) and the Psychophysics Toolbox (psychtoolbox.org). Stimuli were displayed using a modified LED DLP video projector (HP AX325AA Notebook Projection Companion; Hewlett-Packard Co.) with a single near-UV LED (NC4U134A, λ_{max} = 395 nm; Nichia Co., Japan). The projected image was miniaturized and focused onto the retinal photoreceptor layer using the microscope condenser. A 440 nm short-pass dichroic filter (Semrock Inc., Rochester, NY) prevented stimulus light from reaching the photon multiplier tubes. Image size on the retina was 2.1 × 2.8 mm; irradiance 0.1 mW/cm^2. Data were analyzed with custom algorithms in Matlab.

Ferret visual cortex assessment of SF-iGluSnFR.A184S and A184V

All procedures were approved by the Max Planck Florida Institute for Neuroscience Institutional Animal Care and Use Committee and adhered to the standards of the National Institutes of Health. Juvenile female ferrets (*Mustela putorius furo*, Marshall Farms) were used. Animals were housed in a vivarium under 16-hour light/ 8-hour dark cycle. The full methodological details for functional two-photon imaging of ferret visual cortex is previous described in detail [21].

Briefly, juvenile female ferrets aged P21–22 (n = 2) were anesthetized with ketamine (50 mg/kg, IM) and isoflurane (1–3%) delivered in O_2, then intubated and artificially respirated. Atropine (0.2 mg/kg, SC) and a 1:1 mixture of lidocaine and bupivacaine administered subcutaneously in the scalp. Animals were kept at 37°C. A small craniotomy (0.8 mm) was made over primary visual cortex 7–8 mm lateral and 2–3 mm anterior to lambda. AAV2/1.*hSynapsin1*.Cre (Penn Vector Core) was diluted in phosphate-buffered saline (Sigma) and mixed with AAV2/1.*hSynapsin1*-FLEX.SF-iGluSnFR.A184S or A184V for expression in layer 2/3 cortical neurons. Beveled glass micropipettes were lowered into the brain and 400–500 nL of virus were injected over 5 minutes at multiple depths below the pia. Following, the craniotomy was filled with 1% w/v agarose.

After four weeks, ferrets were anesthetized with 50 mg/kg ketamine and 1–3% isoflurane. Atropine (0.2 mg/kg, SQ) and bupivacaine were administered. Animals were kept at 37–38 °C, artificially respirated, and given intravenous fluids. Isoflurane (1–2%) was used throughout the surgical procedure to maintain a surgical plane of anesthesia. ECG, endtidal CO_2, external temperature, and internal temperature were continuously monitored. A custom titanium headplate was implanted on the skull at the viral injection site and the dura retracted to reveal the cortex. A custom insert with a single 5 mm coverglass (0.17 mm or 0.7 mm thickness) was placed onto the brain to gently compress the underlying cortex and dampen biological motion during imaging. The cranial window was hermetically sealed using a stainless-steel retaining ring and Vetbond. Tropicamide Ophthalmic Solution and Phenylephrine Hydrochloride Ophthalmic Solution were applied and contact lenses were

inserted into both eyes. Upon completion of the surgical procedure, isoflurane was gradually reduced and pancuronium (2 mg/kg/hour) was delivered IV to immobilize the animal.

The animal was placed under the microscope 25 cm from the stimulus monitor, with the monitor subtending 130 degrees in azimuth and 74 degrees in elevation. Imaging was performed using a Bergamo II (Thorlabs) running ScanImage 5 or ScanImage 2015[20] (Vidrio Technologies) with dispersion-compensated 950nm excitation provided by an Insight DS+ (Spectraphysics). Average excitation power after the exit pupil of the objective (16×, CFI75, Nikon Instruments) ranged from 25 to 40 mW. Two-photon frame triggers from ScanImage were synchronized with stimulus information using Spike2 (CED). Visual stimuli were generated using PsychoPy[22]. Full-field drifting square-wave gratings (16 directions, 100% contrast, 0.1 cycles/°, 4 cycles/sec., 3 sec. stimulus period followed by 2–3 sec. inter-stimulus interval, plus a blank) were presented to the contralateral eye in a pseudorandom sequence for 8–10 trials.

Images were corrected for in-plane motion using a correlation-based approach (MATLAB). ROI drawing was performed in ImageJ [23]. Fluorescence time-courses were computed as the mean of all pixels within the ROI at each time point and were extracted using Miji[24]. Fluorescence time courses were then synchronized with stimulus information, and visually evoked responses were computed as changes in fluorescence relative to the baseline fluorescence. Peak ΔF/F responses for field ROIs and dendritic spines ROIs were computed using Fourier analysis to calculate mean and modulation amplitudes for each stimulus presentation, which were summed together.

To identify spine SF-iGluSnFR events, ΔF/F traces during individual stimulus trials were smoothed with an exponentially weighted moving average filter (MATLAB) and peaks of possible ΔF/F events were identified. Peak amplitudes were compared to the standard deviation of baseline spine fluorescence values. Identified spine events were those with a peak amplitude greater than the background fluorescence fluctuations by 1, 2 or 3 standard deviations.

Mouse neuronal culture analysis

Primary hippocampal neuron cultures—Primary hippocampal neuron cultures were prepared from embryonic mice (E16) as described previously[25]. Hippocampi were rinsed 3–5 times in Hank's Balanced Salt Solution (HBSS, Life technologies) and digested with trypsin (25 mg/mL, Life Technologies) for 20 min at 37 °C followed by DNase I (1 mg/mL; Roche). Subsequently, the tissue was triturated using cannulas (three times 0.9 mm x 40 mm; three times 0.45 mm x 23 mm) and the solution was passed through a Nylon cell strainer (100 μm; BD Biosciences). The mesh was rinsed with 4–10 mL basal medium eagle (BME, Life technologies) supplemented with 0.5 % glucose (Sigma-Aldrich), 10 % fetal calf serum (FCS), 2 % B-27, and 0.5 mM L-glutamine (all Life Technologies) to collect all cells. After counting, the cells were plated on cover slips in a 24-well cell culture plate at a density of 70,000 cells per 24-well and cultured in a humidified incubator at 37 °C and 5 % CO_2.

Viral vector production—Recombinant AAV2/1 genomes were generated by large scale triple transfection of HEK293 cells as described previously[1]. The adeno-associated virus (AAV) plasmid coding for SF-iGluSnFR.S72A or SF-iGluSnFR.A184V, helper plasmids encoding *rep* and *cap* genes (pRV1 and pH21), and adenoviral helper pFΔ6 (Stratagene) were transfected using the calcium phosphate transfection method. Cells were harvested ~72 h after transfection. To purify the virus, cell pellets were lysed in the presence of 0.5% sodium deoxycholate (Sigma) and 50 units/mL Benzonase endonuclease (Sigma). rAAV viral particles were purified from the cell lysate by HiTrap heparin HP column purification (GE Healthcare) and then concentrated using Amicon Ultra Centrifugal Filters (Millipore) until a final stock volume of 500 μL was reached.

Viral transduction and image acquisition—Primary hippocampal neurons were transduced with AAV2/1.*hSynapsin1*.SF-iGluSnFR.S72A or AAV2/1.*hSynapsin1*.SF-iGluSnFR.A184V on DIV4 and imaged on DIV13. A low amplitude field stimulation (1 msec, 20mA, platinum bar electrodes) was applied to recruit a small fraction (~20%) of neurons. Images were acquired with an EM-CCD camera (frame time 5–50 msec) and a stabilized LED light source of cultures visualized through a coverslip with high NA objective (Zeiss, 63×, 1.4 NA, water). All experiments were performed in Tyrode's solution (1 mL/min) at RT. Low and high affinity versions of SF-iGluSnFR were expressed in a comparable manner.

Glutamate release site localization—Primary hippocampal neurons were transduced with AAV2/1.*hSynapsin1*.SF-iGluSnFR.S72A or AAV2/1.*hSynapsin1*.SF-iGluSnFR.A184V on DIV3–5 and used for experiments on DIV13–18. A low amplitude electrical field stimulation (1 msec., 20 mA, platinum bar electrodes) was applied to activate a small fraction (~20%) of neurons only. Per experiment, stimuli were applied 16–25 times at an inter-stimulus interval of 20–60 sec. Images were acquired with an EM-CCD camera (Hamamatsu ImagEM X1, 8 ms exposure, 125 Hz acquisition rate) attached to an inverted microscope (Nikon T1 Eclipse) using a triggered, stabilized LED light source (Cairn OptoLED with 470 nm excitation wavelength, 470/40 emission filter and 525/50 excitation filter). Cells were imaged through a coverslip with a high NA objective (Zeiss, 63×, 1.4 NA, water). All experiments were performed in saline (1 mL/min, as described above) at room temperature.

In each experiment 30 images were acquired per stimulation trial (20 before and 10 after stimulation). Each of the 30 images was registered to the first image with StackReg Plugin in ImageJ. The image series was then normalized to the average of 5 frames before stimulation to distinguish responding sites (>1) and non-responding structures (~1). For selection of responding sites to be included in the analysis, 10 normalized images subsequent to the stimulus in the first trial were averaged. All spots of increased fluorescence (Supp. Fig. S10c,d) that reached at least 50% of the ΔF/F value of the brightest spot in the image were defined as responding sites and used for further analysis. The spatial extent of glutamate release sites was quantified by extracting a brightness profile based on a line (length: 12–30 pixels, width: 3 pixels) drawn along the underlying neurite. These

profiles were calculated for each stimulation trial and each responding site in an experiment and fitted by Gaussians with Igor Pro 6.3 (Wavemetrics).

In each experiment (n = 6 and 8 for S72A and A184V, respectively, each consisting of 16–25 trials) the mean deviation of the center (X_0 position), the average width and the average amplitude of the fitted Gaussians were calculated per response site and averaged across all experiments and statistically compared by an unpaired Mann-Whitney test, n= 28 and 53 for S72A and A184V, respectively).

Cerebellar granule cell axon experiments and analysis

All protocols were approved by the ethics committee CEEA-Paris1.

Stereotaxic injections—To fluorescently label boutons of parallel fibers, we performed stereotaxic injections of viral vectors expressing SF-iGluSnFR or GCaMP6f into cerebellar vermis. We used the following vectors: AAV-DJ.*hSynapsin1*.SF-iGluSnFR (1.9×10^{13} GC/mL), AAV2/1.*hSynapsin1*.SF-iGluSnFR.S72A (2.6×10^{13} GC/mL), AAV-DJ.*CAG*.FLEX.SF-iGluSnFR.S72A (6.3×10^{12} GC/mL) or AAV-DJ.*hSynapsin1*.GCaMP6f (1.2×10^{13} GC/mL). Mice between 30 and 60 days old (either sex) were deeply anesthetized before surgery with a mixture of hypnotic (ketamine 1.5%, Mérial) and analgesic (xylazine 0.05%, Bayer) anesthetics mixed in NaCl and injected into the peritoneum. A local anesthetic (xylocaine 2% gel, Newpharma) was applied on top of the location of the cranial incision. The anesthetized mouse was then placed on a stereotaxic frame adaptor comprising adjustable ear bars and tooth holder. The skull was then perforated at the injection site with a surgical drill. The vermis was identified using the Paxinos and Franklin mouse brain atlas. The injection of viral constructs in the vermis (100 nL; 6.5 mm caudal to Bregma, lateral 0.2 mm, ventral 3.6 mm and 3.4 mm) was performed by slow infusion (100 nL/min) with steel needles (26G × 50 mm and 36G × 70 mm, Phymep) connected to a pump *via* a catheter and a Hamilton syringe. Injected mice were then kept 2 to 4 weeks to allow transgene expression.

Slice preparation—All protocols were approved by the ethics committee CEEA-Paris1. Cerebellar acute slices were prepared from adult CB6F1 mice (F1 cross of BalbC and C57BL6/J) or Gabra6 mice (B6;129P2-*Gabra6*$^{tm2(cre)Wwis}$/Mmucd) of postnatal day 41 to 123. The mice were killed by rapid decapitation, after which the brains were quickly removed and placed in an ice-cold solution containing (in mM): 2.5 KCl, 0.5 $CaCl_2$, 4 $MgCl_2$, 1.25 NaH_2PO_4, 24 $NaHCO_3$, 25 glucose, 230 sucrose, and 0.5 ascorbic acid bubbled with 95% O_2 and 5% CO_2. Coronal slices were cut from the dissected cerebellar vermis using a vibratome (Leica VT1200S). After preparation, the slices were incubated at 32°C for 30 minutes in the following solution (in mM): 85 NaCl, 2.5 KCl, 0.5 $CaCl_2$, 4 $MgCl_2$, 1.25 NaH_2PO_4, 24 $NaHCO_3$, 25 glucose, 75 sucrose and 0.5 ascorbic acid. Slices were then transferred to an external recording solution containing (in mM): 125 NaCl, 2.5 KCl, 1.5 or 2.0 $CaCl_2$, 1.5 or 1.0 $MgCl_2$, 1.25 NaH_2PO_4, 25 $NaHCO_3$, 25 glucose and 0.5 ascorbic acid, and maintained at room temperature for up to 6 hours. All slice recordings were performed at 36–38°C. In some GCaMP6f experiments 2mM [Ca^{2+}] was used to yield single-stimulus events with sufficient signal-to-noise to measure rise and fall dynamics (Fig. 2f, g; Fig.

S12a), while otherwise 1.5 mM was used to match the [Ca^{2+}] used for all SF-iGluSnFR(1.5 mM). The lower concentration also helped to minimize GCaMP saturation during trains (Fig 2h).

Transmitted light and fluorescence imaging—Parallel fiber and boutons expressing SF-iGluSnFR, GCaMP6f, or loaded with Fluo-5F were identified using an Ultima two-photon scanning scanhead (Bruker Nano Surfaces Division, Middleton, WI, USA) that was mounted on an Olympus BX61W1 microscope, equipped with a water-immersion objective (60×, 1.1 NA, Olympus Optical, Tokyo, Japan) and infrared Dodt-gradient contrast. Two-photon excitation was performed with a pulsed Ti:Sapphire laser (DeepSee, Spectra-Physics, France) tuned to 920 nm for imaging morphology, glutamate and Ca^{2+} fluorescence from genetic probes, and 840 nm for excitation of Fluo-5F (Chameleon, Coherent, USA).

Extracellular PF axonal stimulation was performed using a constant voltage stimulator (Digitimer Ltd, Letchworth Garden City, UK) and a patch pipette (typically with a tip resistance of 4–6 MΩ) filled with ACSF and placed in the molecular layer adjacent to labeled parallel fibers. We monitored the fluorescence of single cerebellar parallel fiber boutons using continuous full field imaging (~7 Hz). The extracellular stimulation intensity was increased until clear fluorescence responses were observed (threshold) following a train of 20–60 voltage pulses (60 μsec duration) at 100 or 300 Hz. The stimulus voltage was then increased by 5V (above threshold), to ensure action potential initiation for each stimulus pulse[14,26] (see Supp. Fig. S15).

Line-scan fluorescence imaging of boutons was performed using a dwell time of 0.8–1.2 μsec per pixel, for 300 to 800 msec. For a single bouton, multiple trials were performed at 0.5 Hz. The line-scan was oriented perpendicular to the axon and bisected the bouton. Background fluorescence ($F_{back}F_{back}$) was measured from 1 μm regions of the line scan with the smallest fluorescent intensity and which did not show any intensity increase during the electrical stimulation. Bouton fluorescence transients were averaged over a 0.5–1 μm width of the line-scan where an evoked transient occurred (transients were identified by eye from averaged line-scan images (n=10–50 trials). The fluorescence traces $\left(F_{(t)}\right)$ were corrected for the background by subtracting F_{back} from the entire trace. In order to calculate a $\Delta F_{(t)}/F_0$ trace, F_0 first was calculated from the average of a 50 msec window of points prior to the stimulus then subtracted from $F_{(t)}$ and then used to scale the difference (see equation (1)).

$$\frac{\Delta F}{F_0}(t) = \frac{F_{(t)} - F_0}{F_0} \quad (1)$$

Analysis of amplitudes and time course were performed and trial-averaged traces 10 pt smoothing. Data were analyzed and presented using custom-written macros in Igor Pro. In order to analyze SF-iGluSnFR responses we analyzed trials in which a fluorescence transient was detected. We denoted a response a “success” if the peak of the fluorescence

response was greater than 3× standard deviation (SD) of the baseline fluorescence fluctuations. To do this, we compared the fluorescence value within 20 msec window around the peak of each transient to the SD of fluorescence values calculated from a 20 msec baseline window on the trial-averaged transient.

The signal-to-noise ratio (SNR) was calculated from the ratio of the peak amplitude of the mean fluorescence trace and the SD of a 20 msec baseline window prior to the start of the electrical stimulation. The peak amplitude of the mean trace was estimated from the peak amplitude of a multi-exponential fit:

$$A(t) = A_{max}\left(1 - e^{-\frac{t-t_0}{\tau_{rise}}}\right)^n \left(A_1 e^{-\frac{t-t_0}{\tau_1}} + A_2 e^{-\frac{t-t_0}{\tau_2}}\right) \quad (2)$$

where t_0 is the start of the peak, τ_{rise} is the rise time constant, τ_1 and τ_2 are the decay time constants, A_{max} is the maximum amplitude in the trace, and A_1 and A_2 are constants that scaled the amplitude of the trace.

Loading of Fluo-5F (400 μM) was achieved using brief whole-cell recordings (1–2 min) of granule cells after which the pipette was removed. AlexaFluor-594 (10 μM) was also included in the intracellular solution to identify loaded boutons. After a 15 min period to allow diffusion and equilibration of the dye, axonal stimulation was performed using an extracellular electrode. The stimulation electrode was positioned close (5–10 μm) to the axon and the intensity of a 50 μsec stimulation voltage pulse was progressively increased until a calcium transient was observed, indicating AP induction. Experiments were performed by setting stimulation intensity 3–4 V above the first stimulation amplitude that generated a fluorescence transient.

The coefficient of variation of the peak of fluorescence responses was calculated from fluorescence traces that were only corrected for PMT bias current ($F_r(t)$) and using the following equation (3):

$$CV = \frac{\sqrt{\sigma_F^2 - \sigma_d^2 - \sigma_{sn}^2}}{\langle \Delta F_r \rangle} \quad (3)$$

The trial-averaged fluorescence transient ($F_r(t)$) and its variance ($\sigma_F^2(t)$) were calculated from 50–70 trials (0.5 Hz) for each bouton. $\langle \Delta F_r \rangle$ is the mean peak amplitude calculated from a 20 msec window around the peak of $\langle F_r(t) \rangle$ corrected by the mean of a 20 msec baseline window prior to the start of the electrical stimulation. σ_F^2 was calculated as the mean variance of $\sigma_F^2(t)$ during the peak window. The dark noise (σ_d^2) was measured without laser illumination. The final variance was estimated after subtracting the expected increased

variance due to photon dependent shot-noise (σ^2_{sn}), which itself was estimated by scaling the fit (equation 2) of $\langle F_r(t) \rangle$ scaled to the average value calculated from the baseline window of $\sigma^2_F(t$.

Fast imaging of SF-Venus-iGluSnFR

Primary rat hippocampal neuron cultures—A mixed cell culture (neurons and glia) was prepared from Sprague-Dawley rat pups (Charles River Laboratories). Briefly, P0 pups (either sex) were decapitated, and the brains were dissected into ice-cold neural dissection solution (NDS, 10 mM HEPES (Sigma) in HBSS (Invitrogen), pH 7.4). Hippocampi were dissected and cut into small pieces to facilitate enzyme digestion. Hippocampi pieces were transferred using a large bore pipette into a 15 mL conical tube and incubated with enzyme digest solution (Papain, Worthington Biologicals) at 37˚C for 30 min. After 30 min., the enzyme solution was removed, and Plating Media (MEM media containing 10% FBS) was added and tissue pieces were triturated resulting in mostly single cells. The cell suspension was filtered using a 45 μm filter. The filtered cell suspension was centrifuged, and the resulting cell pellet was re-suspended with Plating Media and counted.

For electroporation, 1 μg of DNA was mixed with 1×10^6 cells using the Amaxa Nucleofector II instrument. Cells were plated onto coverslips coated with Poly-D-Lysine (Sigma) and kept at 37 °C, 5% CO_2 in PM for ~24 hours and then in NbActiv4 (BrainBits) was added for the duration with medium exchanges every 4 days.

Glutamate uncaging and imaging—Rat hippocampal culture was imaged on DIV19 at room temperature in HEPES buffered Tyrode's solution (145 mM NaCl, 2.5 mM KCl, 10 mM glucose, 10 mM HEPES, 2 mM $CaCl_2$, 1 mM $MgCl_2$, pH 7.4).

Excitation was with a 1030nm, 5 MHz, 190 fsec laser (Menlo Systems, model: Bluecut). Average power was 39mW at the sample. Fluorescence collected at 560/80 nm with a Hamamatsu MPPC detector. The field of view is a 256 μm diameter circle, 1280 pixels across. The bath contained HEPES buffered Tyrode's solution plus 10 μM NBQX and 150 μM RuBi-Glutamate (Tocris). Glutamate uncaging was performed with 420 nm fiber-coupled LEDs (Thorlabs M420F2). The tips of the fibers were imaged onto the sample plane through the same objective used for activity imaging.

Imaging SF-Venus-iGluSnFR at 1030 nm in vivo

Surgical procedure: All surgical procedures were in accordance with protocols approved by the HHMI Janelia Research Campus Institutional Animal Care and Use Committee (IACUC 17–155). An 8-week old female C57BL/6NCrl mouse was anesthetized using isoflurane in oxygen, placed on a heated pad and its head was gently affixed to a head holder using its front teeth. Buprenorphine HCl (0.1 mg/kg) and ketoprofen (5 mg/kg) was administered to the animal *via* subcutaneous injection. A 4.5mm craniotomy (centered ~3.5 mm laterally and ~0.5 mm rostrally from lambda) was opened. We performed 6–8 injections (30nL each, 1 nL/s, 300 μm deep) of viral suspension containing AAV2/1.*hSynapsin1*.FLEX.SF-Venus-iGluSnFR.A184S, final titer 5×10^{11} GC/mL, final

titer 5×10^{11} gc/mL AAV9.*CaMKIIα*.Cre, final titer 1×10^{7} gc/mL, to the left visual cortex. The craniotomy was closed with a 4 mm round cover glass that was fixed to the skull with cyanoacrylate glue. The recordings shown were performed 12 weeks after surgery.

In vivo *imaging*: Imaging was performed with a custom-built two-photon microscope using ScanImage acquisition software (Vidrio Technologies), using 1030 nm excitation (120 fs, 80 MHz, Insight DS+, SpectraPhysics). The mouse was placed in a temperature-controlled plastic tube and its head was immobilized via headbar clamp beneath the water-immersed microscope objective, with a nose-cone delivering 1% vol/vol isoflurane in oxygen. A vertically-oriented screen (ASUS PA248Q LCD monitor, 1920×1200 pixels), was placed 17cm from the right eye of the mouse, centered at 65 degrees of azimuth and −10 degrees of elevation. A high-extinction 500 nm shortpass filter (Wratten 47B-type) was affixed to the screen. Stimuli were drifting square-wave gratings (0.153 cycles per cm, 1 cycle per second, 2 second duration) in 8 equally-spaced directions, spaced by periods of mean luminance, as measured using the microscope detection path. Fluorescence was collected in two channels (500–580nm and 595–685nm) in a custom-built detection system. Isolated dendrites were imaged at 3.4 Hz. Images were aligned to compensate for bidirectional scanning and rolling-shutter motion artifacts using a series of strip-wise registrations implemented in MATLAB code, available upon request. A region of interest was selected manually corresponding to a single dendritic spine. The baseline F0 was calculated as the mean fluorescence intensity over one second prior to stimulus onset.

Simulations of glutamate diffusion—A finite differencing model was used to simulate diffusion of glutamate in water (diffusivity 700 $\mu m^2/s$), with an isotropic spatial resolution of 200 nm, from an initial distribution determined from a 3D intensity pattern than approximates the uncaging light pattern used in our experiments (5 μm spot, 0.8 NA). A time step of 1.43 μs was used, which ensures stability of the simulation with these parameters. The data were fit with custom MATLAB code (glutamateDiffusion.m), available upon request.

Statistical tests

Data are presented as mean with standard error (std. err.) or standard deviation (std. dev.), as noted in each case. All values of *n* are provided; no data were excluded. For comparisons between two datasets, either a two-sided Student's t-test or 2-sided Mann-Whitney U-test (*a.k.a.* Wilcoxon rank-sum test) was used. For comparisons of three or more datasets, Kruskal-Wallis and *post hoc* Dunn's multiple comparisons tests were used.

Supplementary Material

Refer to Web version on PubMed Central for supplementary material.

Acknowledgements

We would like to thank John Macklin (Janelia Research Campus) for 2-photon spectra, and Kim Ritola and Janelia Virus Services for AAV production. Edward Cai was a Janelia Undergraduate Scholar.

References

1. Marvin JS et al. Nature Methods 10, 162–170 (2013). [PubMed: 23314171]
2. Park SJH, Kim I-J, Looger LL, Demb JB & Borghuis BG J Neurosci. 34, 3976–3981 (2014). [PubMed: 24623775]
3. Brunert D, Tsuno Y, Rothermel M, Shipley MT & Wachowiak MJ Neurosci. 36, 6820–6835 (2016).
4. O'Herron P et al. Nature 534, 378–382 (2016). [PubMed: 27281215]
5. Xie Y et al. J. Neurosci. 36, 1261–1272 (2016). [PubMed: 26818514]
6. Bao H et al. Nature Struct. Biol. 23, 67–73 (2016).
7. Rosa JM et al. eLife 4, 728 (2015).
8. Enger R et al. Cerebral Cortex 25, 4469–4476 (2015). [PubMed: 25840424]
9. Jiang R, Diaz-Castro B, Looger LL & Khakh BS J. Neurosci. 36, 3453–3470 (2016). [PubMed: 27013675]
10. Pédelacq J-D, Cabantous S, Tran T, Terwilliger TC & Waldo GS Nature Biotechnol. 24, 79–88 (2006). [PubMed: 16369541]
11. Marvin JS & Hellinga HW Nature Struct. Biol. 8, 795–798 (2001). [PubMed: 11524684]
12. Helassa N et al. Nature (2018). doi:10.1101/233494
13. Dodge FA & Rahamimoff RJ Physiol. 193, 419–432 (1967).
14. Abrahamsson T, Cathala L, Matsui K, Shigemoto R & DiGregorio DA Neuron 73, 1159–1172 (2012). [PubMed: 22445343]
15. Valera AM, Doussau F, Poulain B, Barbour B & Isope PJ Neurosci. 32, 3267–3280 (2012).
16. van Beugen BJ, Gao Z, Boele H-J, Hoebeek F & De Zeeuw CI Frontiers Neural Circuits 7, 95 (2013).
17. Tang S, Liu J, Krasieva TB, Chen Z & Tromberg BJ J. Biomed. Opt. 14, 030508 (2009). [PubMed: 19566289]
18. Kazemipour A et al. bioRxiv 1–29 (2018). doi:10.1101/357269
19. Borghuis BG et al. Imaging light responses of targeted neuron populations in the rodent retina. J. Neurosci. 31, 2855–2867 (2011). [PubMed: 21414907]
20. Pologruto TA, Sabatini BL & Svoboda K ScanImage: flexible software for operating laser scanning microscopes. Biomed. Eng. Online 2, 13 (2003). [PubMed: 12801419]
21. Wilson DE, Whitney DE, Scholl B & Fitzpatrick D Orientation selectivity and the functional clustering of synaptic inputs in primary visual cortex. Nature Neurosci. 19, 1003–1009 (2016). [PubMed: 27294510]
22. Peirce JW PsychoPy--Psychophysics software in Python. J. Neurosci. Meth. 162, 8–13 (2007).
23. Schindelin J et al. Fiji: an open-source platform for biological-image analysis. Nature Methods 9, 676–682 (2012). [PubMed: 22743772]
24. Sage D, Prodanov D, Tinevez J-Y & Schindelin J MIJ: Making Interoperability Between ImageJ and Matlab Possible. ImageJ User Developer Conference 1, 1 (2012).
25. Woitecki AMH et al. Identification of Synaptotagmin 10 as Effector of NPAS4-Mediated Protection from Excitotoxic Neurodegeneration. J. Neurosci. 36, 2561–2570 (2016). [PubMed: 26936998]
26. Silver RA, Cull-Candy SG & Takahashi T Non-NMDA glutamate receptor occupancy and open probability at a rat cerebellar synapse with single and multiple release sites. J. Physiol. 494 **(** Pt 1**),** 231–250 (1996). [PubMed: 8814618] **(),**
27. Mena MA, Treynor TP, Mayo SL & Daugherty PS Blue fluorescent proteins with enhanced brightness and photostability from a structurally targeted library. Nature Biotech. 24, 1569–1571 (2006).
28. Goedhart J et al. Structure-guided evolution of cyan fluorescent proteins towards a quantum yield of 93%. Nature Commun. 3, 751 (2012). [PubMed: 22434194]
29. Nagai T et al. A variant of yellow fluorescent protein with fast and efficient maturation for cell-biological applications. Nature Biotech. 20, 87–90 (2002).

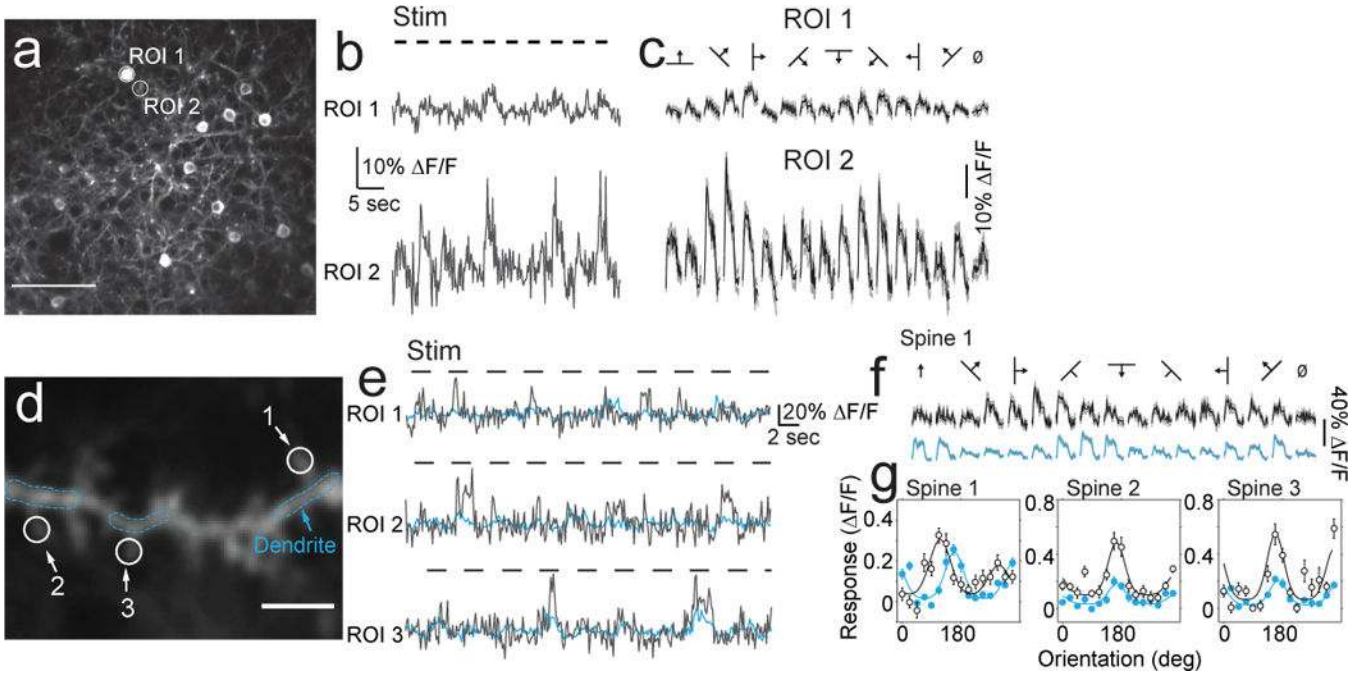

Fig. 1. SF-iGluSnFR.A184S detects orientation selective glutamate transients in ferret visual cortex.

a) Two-photon standard-deviation projection of SF-iGluSnFR.A184S expressed in ferret visual cortex (190 μm depth, scale bar 100 μm). b) Fluorescence changes (ΔF/F) to randomly oriented drifting gratings (dashed lines) shown for both a soma (ROI 1) and nearby neuropil (ROI 2) in an individual trial. c) Trial-averaged stimulus-evoked responses (shown for ROIs 1 and 2) reveal robust orientation tuning. Neuropil peak amplitudes were greater (~30–40% ΔF/F) than that for soma ROIs (~5–10% ΔF/F). Responses shown as the mean (black) and standard error (grey) over 10 presentations of each grating direction and a blank (grey screen) period. d) Two-photon standard-deviation projection of an isolated dendritic segment with active spines revealed with SF-iGluSnFR.A184S (scale bar 5 μm). e) Fluorescence (ΔF/F) during visual stimulation for individual dendritic spines (grey) and nearby dendritic segments (cyan). f) Same as in (c) for an individual dendritic spine (grey) and nearby dendrite. Spines exhibit selective and robust responses to drifting gratings. Each response is shown as the mean (black) and standard error (grey) over 8 presentations of each grating direction and a blank (grey screen) period. Dendritic spine responses can have differential tuning from nearby dendritic segments (cyan). (g) Peak responses are plotted as a function of stimulus direction, showing robust selectivity of spines and larger responses than nearby dendritic segments. Images were collected at 30 Hz. Data points are average of 8 experiments, with error bars showing SEM. Measurements for a-c were repeated for 47 ROI pairs across 3 fields of view with similar results. Measurements for d-f were repeated from a total of 76 spine ROIs from 3 dendrites across 3 fields of view with similar results. See also Supp. Video 1.

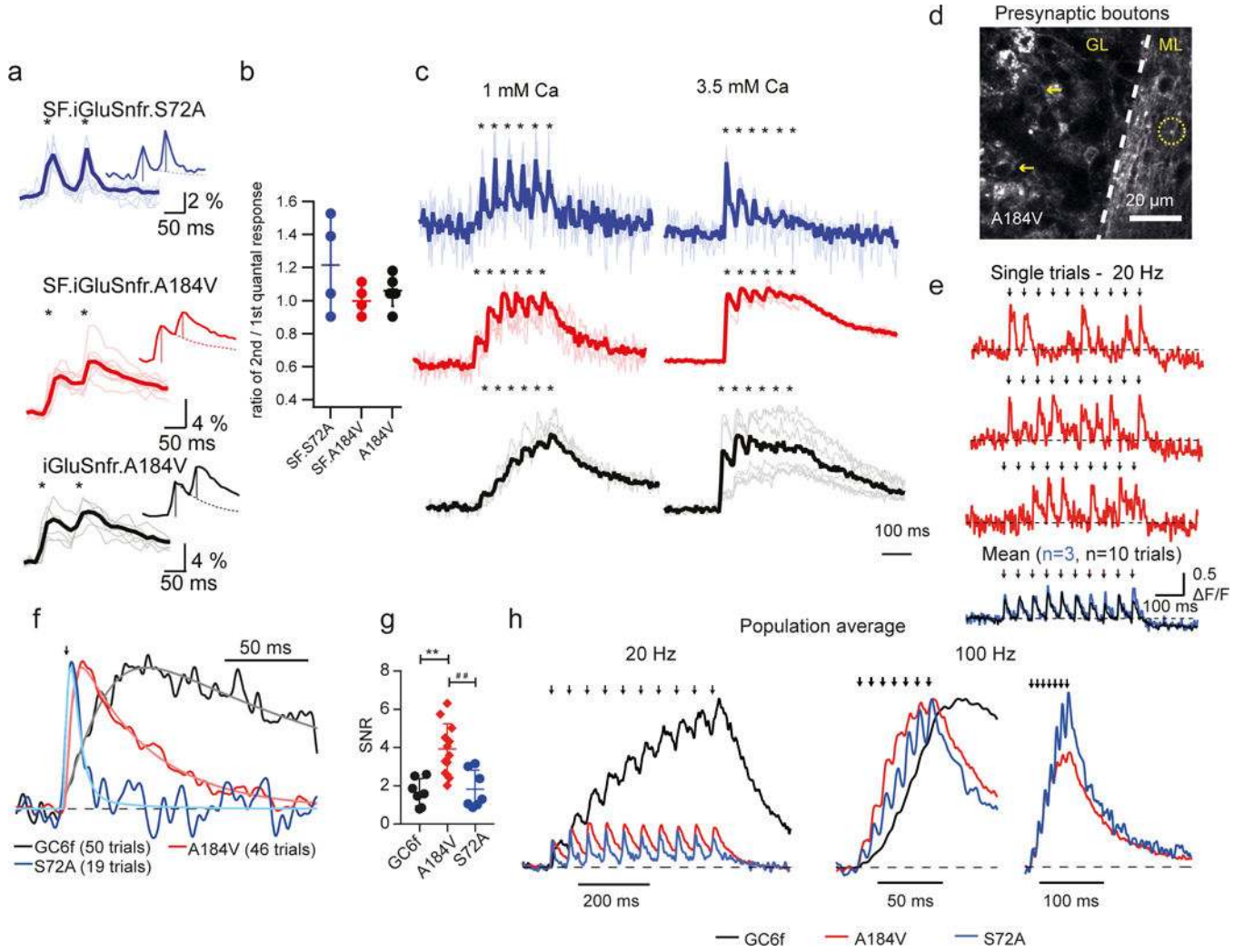

Fig. 2. SF-iGluSnFR.S72A permits resolution of multiple glutamate release events in cultured neurons and in single cerebellar granule cell boutons, acting as a proxy for high-frequency activity.

a-c) *Cultured mouse hippocampal neurons.* a) Averaged traces of SF-iGluSnFR.S72A (blue, n=4), SF-iGluSnFR.A184V (red, n=4) and iGluSnFR.A184V (black, n=5) response to paired electrical stimuli (100 msec interval). Light traces represent individual trials throughout the figure; dark traces show average. Asterisks indicate times of stimulation. Insets show averaged response trials in which the first and second stimulus each trigger quantal release events. b) Ratio of the amplitudes of the second over the first fluorescent responses to two consecutive quantal glutamate release events. The ratio is slightly larger than unity most likely due to the fact that slight cross-talk from neighboring release sites adds to the second response. Dots denote individual experiments, horizontal and vertical lines indicate mean and standard deviation, respectively. c) The faster off-rate of S72A allows observation of short-term plasticity during 20 Hz trains of synaptic activity. The conversion of facilitation of vesicle release to depression with increased extracellular calcium is most clearly reported by SF-iGluSnFR.S72A (blue, similar results were obtained in 5 independent experiments) when compared to SF-iGluSnFR.A184V (red, 5 experiments)

and iGluSnFR.A184V (black, 4 experiments). Traces have been scaled to maximal response for clarity. d-g) *Cerebellar granule cell boutons*. d) Two-photon fluorescence image of granule cells (arrows) and its axonal boutons (circle) expressing SF-iGluSnFR.A184V (GL, granular layer; ML, molecular layer) in an acute brain slice. e) Single trials (red) and mean traces (blue, average of 3 trials; black, average of 10 trials) of SF-iGluSnFR.A184V responses to 20 Hz extracellular stimulation. Similar results in 11 boutons. f) Normalized averaged fluorescence traces from single boutons expressing GCaMP6f (GC6f; black, 2 mM $[Ca^{2+}]_e$), SF-iGluSnFR.A184V (A184V; red, 1.5 mM $[Ca^{2+}]_e$) and SF-iGluSnFR.S72A (S72A;blue, 1.5 mM $[Ca^{2+}]_e$) in response to single APs. Results repeated in n=10 boutons expressing GC6f; n=12, A184V; n=7, S72A. g) Summary plot of signal-to-noise ratio (SNR; mean ± SD; n boutons=7, GC6f; n=12, A184V; n=7, S72A; ** P=0.0033, ## P=0.0096). Multiple comparisons were performed with the Kruskal-Wallis test and Dunn's multiple comparisons test. h) Population-averaged response at same calcium concentration to 20 Hz stimulation normalized to the peak of the first response (right; n boutons=5, GC6f, 1.5 mM $[Ca^{2+}]_e$; n=17, A184V; n=6, S72A) and population-averaged response at same calcium concentration to 100 Hz normalized to the maximum amplitude (middle; n boutons=9, GC6f 1.5 mM $[Ca^{2+}]_e$; n=9, A184V; n=9, S72A) or to the peak of the first response (right; n boutons=9, A184V; n=9, S72A). Black arrows indicate 60 μsec extracellular voltage pulse times.

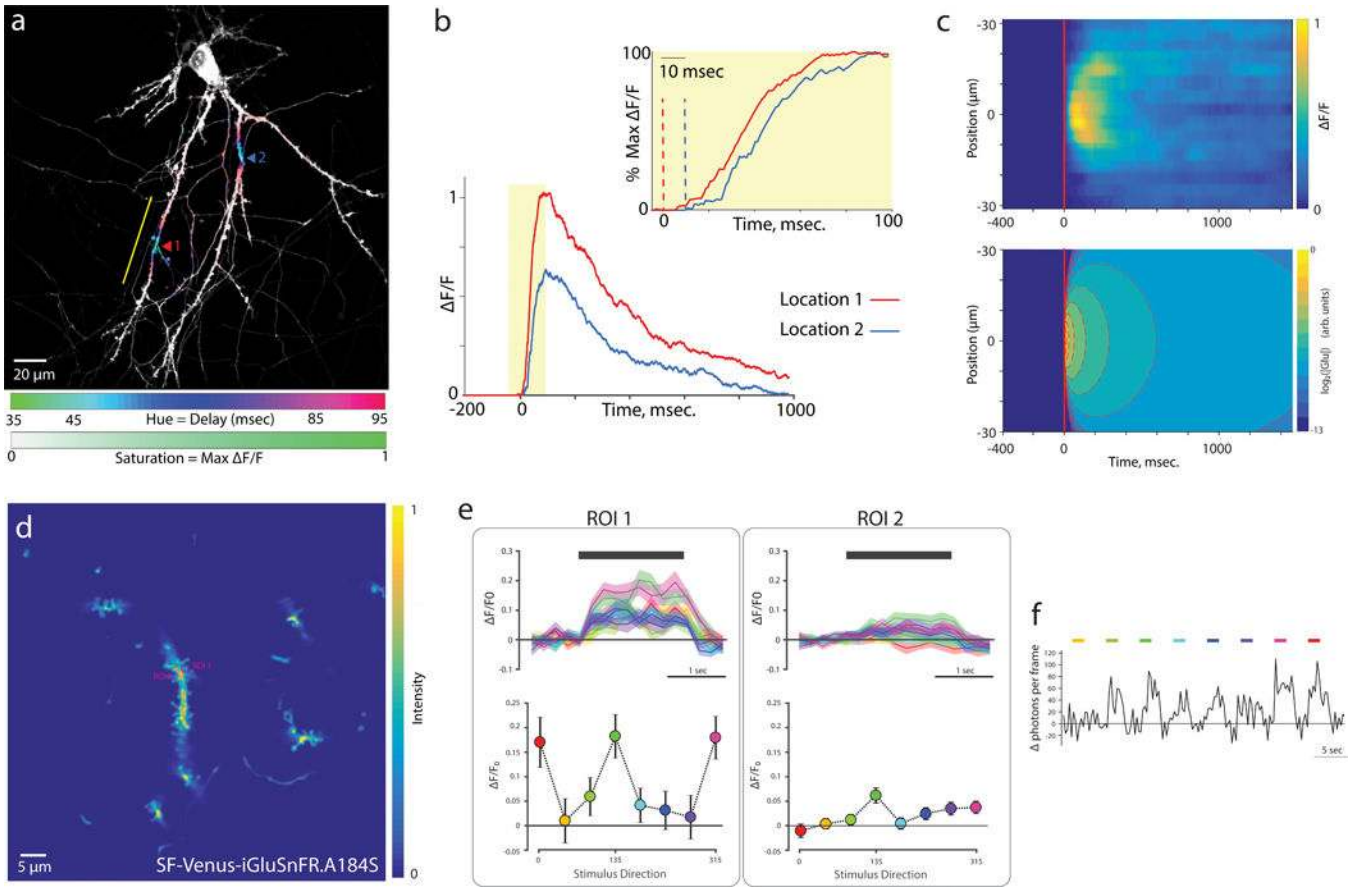

Fig. 3. Utility of SF-Venus-iGluSnFR in cultured neurons and *in vivo*.

(a-c) High-speed (1016 Hz frame rate) two-photon imaging of a cultured neuron expressing SF-Venus-iGluSnFR.A184V. a) RuBi-glutamate was uncaged for 10 msec. at each of two 5-micron spots (arrowheads) on two adjacent dendrites (Supp. Video 2). Color saturation denotes the glutamate transient amplitude; grey tones indicate no evoked response. Color hue denotes response timing (see scale bars). The yellow line indicates the axis of the kymograph shown in (c). Representative example of 4 trials. b) Recorded traces at the centers of the uncaging locations shown in (a). c) Top: Kymograph showing the response amplitude over time along the dendrite surrounding uncaging location 1. Traces are approximate maximum-likelihood solutions[18] for a spatially multiplexed recording acquired with a high-power 1030 nm fiber laser. These recordings show a single trial without averaging. Bottom: simulation (Methods) of diffusion of glutamate at the surface of a planar coverslip surrounded by 3D solution, following uncaging in a 5 μm spot with a 0.8 NA beam at time 0. Intensity scale is log-transformed. (d-f) Recording of visually-evoked spine transients in isolated SF-Venus-iGluSnFR.A184S labeled dendrites in mouse visual cortex, imaged at 1030 nm excitation. See also Supp. Video 3. d) Motion-aligned average image. e) Mean responses (top) and tuning curves (bottom) of ROIs indicated in d, for 20 trials of each of the 8 oriented moving grating stimuli. Dark lines/markers denote mean, shaded regions/error bars denote SEM. Black bar denotes the stimulus period. f) pixel intensity of ROI 1 for eight consecutive stimulus presentations of different directions, illustrating detectable

responses in single trials. Colored bars denote stimuli as in (e). The spine response is selective to the stimulus orientation. (d-f) representative example of 7 mice.